Preprints, 4th IFAC Conference on
Advances in Proportional-Integral-Derivative Control
Almería, Spain | June 12-14, 2024

# Feedforward PID Controller Design For a Parabolic Trough Solar Collector ⋆

**Marta Leal** [*,**] **José Domingo Álvarez** [*,**]
**María del Mar Castilla** [*,**] **Manuel Berenguel** [*,**]

[*] *CIESOL, Solar Energy Research Centre, University of Almería-ceiA3, Ctra. Sacramento s/n, La Cañada de San Urbano, Almería 04120, España.*
[**] *Department of Informatics, University of Almería- ceiA3, Ctra. Sacramento s/n, La Cañada de San Urbano, Almería 04120, España, (e-mail: marta.leal@ual.es, jhervas@ual.es, mcastilla@ual.es, beren@ual.es)*

**Abstract:** Distributed parameter systems (DPS) are widely recognised in the process industry. An innovative feedforward control strategy for the DPS of a parabolic trough collector (PTC) has been developed with the aim of rejecting disturbances. This feedforward is designed on a transfer function based on a semi-physical model. This transfer function includes an irrational term that models the resonance dynamics in the system response. For validation, this approach is compared with a proportional-integral (PI) design and other existing feedforward designs in literature. The results show that the proposed approach significantly improves the system performance in the presence of disturbances addressing system dynamics at medium and high frequencies.

*Keywords:* Feedforward control, PID control, Distributed parameter systems, Resonance

## 1. INTRODUCTION

Distributed parameter systems (DPS) are commonly found in the process industry, such as heat exchangers, tubular and packed bed reactors and solar collector systems. These systems are typically represented using partial differential equations (PDE) and have been a subject of research since the mid-20th century, as evidenced by the works of Cohen and Johnston (1956), up to more recent research such as Song et al. (2020).

To address DPS and their associated challenges, various strategies are employed. The first involves simplifying fixed-parameter systems using ordinary differential equations (ODE). This makes it easier to obtain first or second order transfer functions through the Laplace's transform for tuning Proportional Integral Derivative (PID) controllers (Camacho et al. (2007)). However, this means that relevant system dynamics are not taken into account when tuning the PID controller. Alternatively, a higher-order transfer function can be derived for application in more complex control systems, such as model predictive control (MPC) Johansen et al. (2000), but this sacrifices the physical interpretation of the parameters.

The paper Curtain and Morris (2009) highlights notable distinctions in the analysis of rational and irrational transfer functions, particularly in their poles and zeros. Focusing on the transfer functions derived from PDE, the location of the poles and zeros depends crucially on the choice of boundary conditions. Various instances are provided that use irrational functions operating under diverse boundary conditions to apply different control strategies (e.g. heated rod, a vibrating string, a flexible beam).

In the context of solar energy systems, irradiance is the predominant disturbance that affects the performance of the parabolic trough collector (PTC). Traditional control strategies, based on simplified global parameter models, do not address the specific problems posed by the distributed nature of the collector and how irradiance affects the dynamic behaviour of the system. Feedback control can be a powerful choice to open-loop control, but it does not prevent by itself the nondesirable behaviour that the disturbances cause at the process output. Feedforward control complements the control action to be taken before any disturbance affects the process output behaviour. Today, feedforward is implemented in most distributed control systems and is also used in simple control problems to improve performance (Guzmán and Hägglund (2011)).

The main contribution of the present research is the development of a specific methodology to design a feedforward controller that accounts for the irrational term by modelling the resonance dynamics in the system response of a PTC. This approach aims to achieve more effective disturbance rejection compared to other feedforward schemes present in the literature calculated from low-order transfer functions obtained through the system open-loop response.

The rest of the document is structured as follows: Section 2 presents a brief description of the DPS model employed in

⋆ This work has been funded by the National R+D+i Plan Project PID2021-126889OB-I00 of the Spanish Ministry of Science and Innovation and EIE funds.

© 2024 the authors. Accepted by IFAC for publication under a Creative Commons License CC-BY-NC-ND

the control design. Section 3 elaborates on the feedforward design. The results of applying the proposed methodology are presented in Section 4. Finally, Section 5 provides a summary of the main conclusions and future research.

## 2. CONTROL STRATEGY

### *2.1 System model*

DPS can be expressed in terms of transfer functions when linearised, as described in Bellman and Cooke (1963) and Ramanathan et al. (1989). These appear in (1), which consists of low-order rational transfer functions, $P(s)$ and $Q(s)$, and the irrational transfer function $R(s)$. $P(s)$ is the part of the system without resonance dynamics and $R(s)$ characterises the transfer function modelling resonance dynamics. The parameter $\theta$ is often associated with the process residence time.

In this paper, a detailed mathematical derivation leading to $G(s)$ is not included. However, the interested reader can refer to Álvarez et al. (2009). Álvarez et al. (2012) introduced (1), which enables the derivation of first-order rational equations from $G(s)$. These equations are used to replicate the open-loop step response of the system, which typically lacks resonance effects at medium to high frequencies. Alternatively, higher-order equations can be derived to account for resonances using a rational approximation of $G(s)$. When aiming for a high closed-loop bandwidth, controllers based on first-order models typically need to be detuned. However, high-order models require more complex control methods.

$$G(s) = P(s) \underbrace{\left(1 - e^{-\theta s} \underbrace{\left(\frac{-\beta s + 1}{\tau s + 1}\right)}_{Q(s)}\right)}_{R(s)} \tag{1}$$

### *2.2 Proposed control structure*

Álvarez et al. (2012) describe a methodology that has been shown to be easy and effective. They suggest using the irrational transfer function provided by (1) for control design purposes. A simple PID controller can be designed for the transfer function without resonance dynamics, $P(s)$, using any of the existing methods in the literature, such as those proposed in Ziegler and Nichols (1942), Rivera et al. (1986) or Skogestad (2003). The resonance dynamics introduced by $R(s)$ can be dealt with with a specific filter. In Álvarez et al. (2009) is also shown that in the PTC the transfer function that related the control variable (volumetric flow) to the controlled variable (the output temperature) has a similar structure that in (1), with a low order rational transfer function plus a function that model the resonance behaviour.

When designing a disturbance rejection controller, the objective is to combine the classic PID controller with a feedforward control structure. Feedforward control attempts to compensate for disturbances before they impact the system. This approach must take into account the effect of resonances present in the system, which enhances

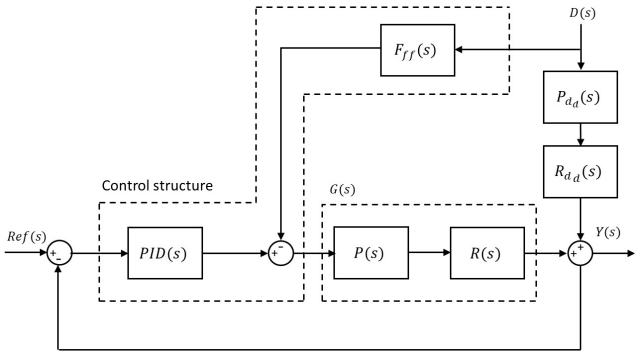


Fig. 1. Proposed control structure

the ability of the feedforward control to counteract disturbances at specific frequencies. Fig. 1 illustrates the proposed control structure, where $Y(s)$, $Ref(s)$ and $D(s)$ represent the closed-loop output, reference, and disturbances signal, respectively. The transfer functions $G(s)$, $P(s)$, and $R(s)$ correspond to (1). $P_{d_d}(s)$ and $R_{d_d}(s)$ are the transfer functions that model the disturbance and they are showed in (6). Finally, $PID(s)$ is a PID controller and $F_{ff}(s)$ is the feedforward designed specifically from the frequency response of $R(s)$.

## 3. FEEDFORWARD DESIGN PROPOSAL

To validate the proposed methodology, we present an implementation example applied to the case study discussed in this work: a solar plant that uses PTC technology. The following non-linear model can be used to model this plant, which describes the energy balance in the fluid by using (2) and in the pipe (subscript $w$) by using (3).

$$A_i \rho C \frac{\partial T}{\partial t} + \dot{q} \rho C \frac{\partial T}{\partial x} = \pi D_i h_i (T_\omega - T) \tag{2}$$

$$\rho_\omega C_\omega A_o \frac{\partial T_\omega}{\partial t} = In_o G - \pi D_o h_o (T_\omega - T_g) - \pi D_i h_i (T_\omega - T) \tag{3}$$

The definition of the parameters given in (2) and (3) is presented in Table 1. Due to the lack of space, not all mathematical developments are presented in this work, but, for interested readers, a comprehensive description of the plant, together with a detailed presentation of the physical parameters, is available at Camacho et al. (2007). This type of model is classified as semi-physical and is characterised by the incorporation of prior knowledge of the system. They represent a hybrid approach, combining elements of physical and empirical models and incorporating adjustable parameters that are amenable to physical interpretation. The simulations carried out in this study were performed to obtain a linear approximation of (2) and (3) of the non-linear model. To achieve the linear approximation of the non-linear parts mentioned above, the Taylor series development was implemented. Subsequently, (4) and (5) were obtained by simple simplification.

$$\frac{\partial T}{\partial t} = -(v - v_s)\frac{dT_s}{dx} - v_s \frac{\partial T}{\partial x} + \frac{1}{\tau_1}(T_w - T) \tag{4}$$

$$\frac{\partial T_w}{\partial t} = I\gamma - \frac{1}{\tau_2}(T_w - T_g) - \frac{1}{\tau_{12}}(T_w - T) \tag{5}$$

Where $\tau_1$, $\tau_2$ and $\tau_{12}$ are time constants relating the temperatures and $\gamma$ is an auxiliary parameter.

The work of Álvarez et al. (2009) presents an exhaustive development of the previous expressions, ultimately leading to individual Single Input Single Output (SISO) transfer functions relating the input variables: the input temperature, the ambient temperature, the solar irradiance and the fluid velocity ($T(0,s)$, $T_g(s)$, $I(s)$ and $v(s)$), to the output variable, $T(L,s)$, assuming constant of the rest of the signals. In this paper, we focus on the transfer functions that relate solar irradiance and fluid velocity, since the other disturbances can be considered to be almost constant during the operation of the system. These transfer functions can be used to formulate control strategies, either by feedback or feedforward, and are presented in a generalised form in (6) and (7).

$$\frac{T(L,s)}{I(s)} = \frac{k_I}{s^3 + a_1 s^2 + a_2 s + a_3} \cdot \left(1 - e^{-\frac{L}{v_s}s}\left(K_D \frac{-\beta s + 1}{\tau s + 1}\right)\right) \tag{6}$$

$$\frac{T(L,s)}{v(s)} = \frac{k_v(b_0 s + 1)}{s^2 + a_1 s}\left(1 - e^{-\frac{L}{v_s}s}\left(\frac{-\beta s + 1}{\tau s + 1}\right)\right) \tag{7}$$

Where $k_I$, $k_v$ refer to static gains, the coefficient $b_0$ is a zero that appear in (7), whereas the coefficients $a_1$, $a_2$, $a_3$ refer to the poles appearing in (6) and (7). Note that $a_1$, $\beta$ and $\tau$ in (6) and (7) are general parameters and do not have the same value. Finally, $K_D$ is a coefficient that multiplies the part referring to $Q(s)$ and in the case of a PTC the parameter $\theta$ is equal to the residence time of the fluid inside the pipe, that is, $\theta = L/v_s$

The only variable that can be manipulated in this kind of system is the fluid velocity. In this work, the control variable is the flow rate or volumetric flow, $\dot{q}(s)$, which can be easily obtained by multiplying the fluid velocity by the internal area of the pipe, $A_i$. For the design of the control schemes, the transfer function that relates the volumetric flow, $\dot{q}(s)$, to the output temperature, $T(L,s)$, described in (8) and the transfer function that relates the solar irradiance, $I$, to $T(L,s)$, presented in (9), have been obtained by means of reaction curve tests in simulation

Table 1. Model parameters of a solar tube heat exchanger

| Parameter | Description | Unit |
|---|---|---|
| $A_i$ | Inner pipe area | $m^2$ |
| $A_o$ | Outer pipe area | $m^2$ |
| $C$ | Fluid specific heat capacity | J/(kg°C) |
| $C_\omega$ | Pipe material heat capacity | J/(kg°C) |
| $D_i$ | Inner pipe diameter | m |
| $D_o$ | Outer pipe diameter | m |
| $G$ | Opening of the collector | m |
| $h_i$ | In-pipe convective HTC | W/($m^2$°C) |
| $h_o$ | Convective HTC outside pipeline | W/($m^2$°C) |
| $I(t)$ | Solar irradiance | W/$m^2$ |
| $L$ | Pipe length | m |
| $n_0$ | Optical efficiency of the collector | – |
| $\dot{q}(t)$ | Volumetric flow | $m^3$/s |
| $\rho$ | Fluid density | kg/$m^3$ |
| $\rho_\omega$ | Pipe density | kg/$m^3$ |
| $T(x,t)$ | Fluid temperature | °C |
| $T_g(t)$ | Ambient temperature | °C |
| $T_\omega(x,t)$ | Pipe temperature | °C |
| $v(t)$ | Fluid velocity | m/s |

with a non-lineal model that implement in (2) and (3). Equations (6) and (7) become (9) and (8) respectively.

$$\frac{T(L,s)}{\dot{q}(s)} = \frac{k_g}{\tau_g s + 1} e^{-t_{r,g}s} \tag{8}$$

$$\frac{T(L,s)}{I(s)} = \frac{k_d}{\tau_d s + 1} \tag{9}$$

Where $k_g$ and $k_d$ refer to the static gains in $m^3$/(s°C) and W/($m^2$°C), respectively, whereas $\tau_g$ and $\tau_d$ are the time constants in s and $t_{r_g}$ is the time delay in s.

A comparison of four control systems will be conducted. The first system is a Proportional-Integral (PI) controller, which has been tuned by using (8). The tuning was performed using two different methods designed for first-order equations with delay. The purpose of this approach is to validate the applicability of the proposed feedforward control approach in the context of various tuning methods. The first tuning method is the one proposed in Ziegler and Nichols (1942) and the second is the SIMC method (Skogestad (2003)) because of their different approaches and being considered the most interesting in this study after comparing them with other tuning methods appearing in the literature (Åström and Hägglund (2009)).

The second scheme involves incorporating a feedforward with the PI controller design. The function $F_{ff}(s)$, shown in Fig. 1, is derived from (8) and (9) obtained during the open-loop analysis, resulting in the formulation of (10). The structure of this design is a lead-lag feedforward without time delay that is not considered to avoid problems with delay inversion.

$$F_{ff}(s) = \frac{k_d}{k_g}\frac{\tau_g s + 1}{\tau_d s + 1} \tag{10}$$

This scheme constitutes a classical feedforward design solution that can be improved with other tuning rules such as the one developed (Guzmán and Hägglund (2011)). This rule relies on adjusting the feedforward gain and the time constant, $\tau_d$, to decrease the overshoot in the output of the system and minimise the value of the integrated absolute error (IAE). This rule is the third control scheme presented in this study and the compensator parameters are calculated as follows in (11) and (12), taking into account that in the specific case under study $t_{r,d} = 0$ and setting $\beta_{ff} = \tau_g$.

$$F_{ff_i}(s) = k_{ff}\frac{\beta_{ff} s + 1}{\tau_{ff} s + 1} \tag{11}$$

$$\tau_{ff} = \begin{cases} \tau_d & t_{r,g} - t_{r,d} \leq 0 \\ \tau_d - \dfrac{t_{r,g} - t_{r,d}}{1.7} & 0 < t_{r,g} - t_{r,d} < 1.7\tau_d \\ 0 & t_{r,g} - t_{r,d} \geq 1.7\tau_d \end{cases} \tag{12}$$

The compensator gain, $k_{ff}$, is calculated by using (13) and (14).

$$k_{ff} = \frac{k_d}{k_g} - \frac{k_p}{\tau_i} IE \tag{13}$$

$$IE = \begin{cases} k_d(\tau_{ff} - \tau_d) & t_{r,d} \geq t_{r,g} \\ k_d(t_{r,g} - t_{r,d} - \tau_d + \tau_{ff}) & t_{r,d} < t_{r,g} \end{cases} \tag{14}$$

Figures 2 and 3 show the magnitude bode diagram of the transfer function that relates the disturbance (solar irradiance) to the controlled variable (the output temperature)

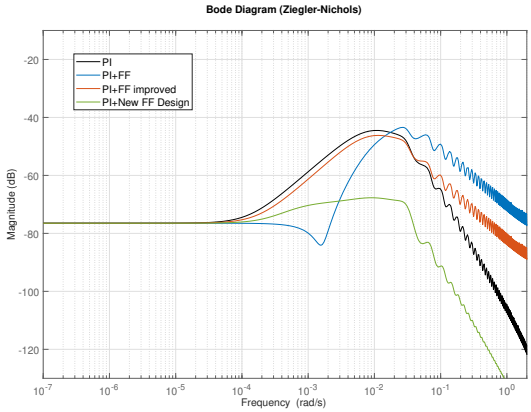


Fig. 2. Bode magnitude plot comparing four control schemes (Ziegler-Nichols Tuning).

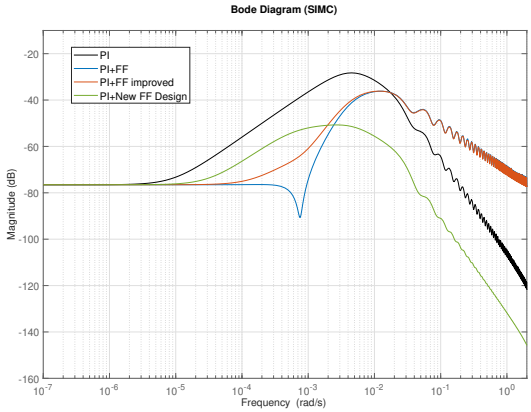


Fig. 3. Bode magnitude plot comparing four control schemes (SIMC Tuning).

for the PI tuning schemes. The black line corresponds to the first control scheme, only the PI controller, the blue represents the second where the feedforward controller is incorporated to the control scheme and the orange represents the third with the improved feedforward.

Note that, incorporating the lead-lag feedforward into the system control results in a decrease in magnitude at low frequencies, which is the aim of designing a feedforward controller. However, as a consequence of using low order transfer functions approximations, (8) and (9), to calculate the feedforward controller instead of more accurate transfer functions, (6) and (7), that take into account resonance dynamics, at medium and high frequencies the magnitude increases and the resonance modes are emphasised. This phenomenon is common to both tuning techniques and can significantly affect the stability and system time response, posing an additional challenge to achieving the established control objectives.

With the intention of improving the frequency behaviour and addressing the cancellation of significant resonances, the formulation of a new feedforward design is proposed. This design is based on the SISO transfer functions associated with (6) and (7) using the rational part of these transfer functions. The new transfer function for the feedforward is defined in (15) where a filter, $F(s)$, is added. This filter is composed of a pole in $s = 0$ to counteract the zero in $s = 0$ that appears in (7) and a zero since the irrational part that models the resonance dynamics in (6) and (7) is slightly different. $a_0$ is a fitting parameter between the difference of the system transfer function in (7) and the disturbance in (6). The value of this parameter can be adjusted to make the feedforward response more or less aggressive in terms of disturbance rejection.

$$F_{ff_{new}} = \overbrace{\frac{k_I}{s^3 + a_1 s^2 + a_2 s + a_3}}^{P_{d_d}(s)} \underbrace{\frac{1}{A_i} \frac{k_v(b_0 s + 1)}{s^2 + a_1 s}}_{P(s)} \underbrace{\frac{s + a_0}{s}}_{F(s)} \tag{15}$$

When analysing the frequency response of the proposed feedforward design, represented by the green line in Figs. 2 and 3, a more attenuated signal is perceived at any frequency, without the presence of the magnitude peak that characterised the lead-lag feedforward response. In addition, the magnitudes at medium and high frequencies are lower than using the previous feedforward, which implies that the resonance modes will affect the system output less than in the previous design.

## 4. RESULTS

After applying the methodology described in Section 3, the results obtained for the specific case study are shown. Firstly, the low-order transfer function approximations relating $I(s)$ and $q(s)$ to the outlet temperature, $T(L, s)$, see (8) and (9), are presented:

$$\frac{T(L,s)}{q(s)} = \frac{-7.15 \cdot 10^4}{148.22s + 1} e^{-22s} \tag{16}$$

$$\frac{T(L,s)}{I(s)} = \frac{0.102}{323.81s + 1} \tag{17}$$

The other disturbances of the system, $T_g(s)$ and $T(0, s)$, were assumed to be constant for the simulations performed in this work. The results obtained for the PI controller parameters for the Ziegler-Nichols rules are: a proportional gain $k_p = -8.48 \cdot 10^{-5}$ m$^2$/(s°C) and a time integral $\tau_i = 73.26$ s and for the SIMC rules considering a $\tau_{bc} = 0.9 \cdot \tau_g$ s are: a proportional gain $k_p = -2.26 \cdot 10^{-5}$ m$^2$/(s°C) and an integral time $\tau_i = 155.55$ s are obtained.

The transfer function obtained by applying the classical feedforward structure outlined in (10) in shown in (18).

$$F_{ff}(s) = -1.43 \cdot 10^{-6} \frac{148.22s + 1}{323.81s + 1} \tag{18}$$

The transfer function obtained by applying the improved feedforward structure outlined in (11) in shown in (19) and (20) to each tuning method study.

$$F_{ff_i}(s) = -3.57 \cdot 10^{-7} \frac{148.22s + 1}{310.87s + 1} (\text{Z} - \text{N}) \tag{19}$$

$$F_{ff_i}(s) = -1.34 \cdot 10^{-6} \frac{148.22s + 1}{310.87s + 1} (\text{SIMC}) \tag{20}$$

However, if the methodology proposed in this work to design the feedforward controller is applied, the following (21) is obtained for the feedforward controller.

$$F_{ff_{new}} = \frac{38.2640s^2 + 0.6297s}{(-3.35s^3 - 0.085s^2 - 0.0005s)1 \cdot 10^9} \cdot \frac{s + 0.00045}{s} \quad (21)$$

Critical to the application of this strategy is the correct choice of $a_0$, whose value has been obtained by trial and error. Fig. 4 shows the control system response when applying this strategy for different values of $a_0$. Solar irradiance saved during one operation day in the solar plant for which the model is available is considered for simulations. Only the response for the SIMC method is shown due to a lack of space. Fig. 4 [1] shows how the variation of $a_0$ changes the response of the output and control signal such that the higher the value of $a_0$, the better IAE but the higher Total Variation (TV) index, indicating that better reference tracking is penalised with a more aggressive control signal. The value of $a_0$ is chosen by finding a trade-off solution between these two features (reference tracking and control signal variation).

The temporal results of the four control systems, the PI controller, the PI with the classical feedforward scheme, the PI with improved feedforward and the PI with the proposed new feedforward design, taking into account the resonances, are shown in detail in Figs. 5 and 6 for both tuning methods. Table 2 shows a comparison of IAE, which is used as a metric to evaluate the deviation between the system output and the reference over time. Table 3 shows a comparison of TV, which is used as a metric to evaluate the control action effort.

Table 2. IAE of Four Control Schemes

| Tuning method | PI | PI+FF | PI+FF$_i$ | PI+ New FF |
|---|---|---|---|---|
| Ziegler-Nichols | 91.240 | 52.524 | 68.936 | 32.808 |
| SIMC | 803.263 | 349.796 | 155.666 | 133.426 |

Table 3. TV of Four Control Schemes

| Tuning method | PI | PI+FF | PI+FF$_i$ | PI+ New FF |
|---|---|---|---|---|
| Ziegler-Nichols | 1.462 | 4.358 | 1.420 | 1.790 |
| SIMC | 0.886 | 7.580 | 3.569 | 1.310 |

Figures 5 and 6 show in the upper graph the time response of the output temperature, whereas in the lower graph only the control signal is shown, which refers to how the volumetric flow varies over time to maintain the output temperature constant. It can be seen that the output temperature for the first control scheme (black line) has large oscillations over the reference reference, which has been considered as 230 °C since the results are shown in a general way. The addition of the classic feedforward scheme, the blue line, results in a more aggressive control signal, leading to recurrent oscillations for both tuning rules. This is caused by the excitation of resonances at intermediate frequencies, as shown in Figs. 2 and 3.

Regarding the output temperature evolution shown in Fig. 5, it is worth noting that this tuning method is more aggressive in rejecting disturbances. As a result, it can cause oscillations, which, despite having a smaller error with respect to the reference, may affect the stability of the system. The SIMC tuning method (refer to Fig. 6)

[1] Please note that for a better understanding the volumetric flow is expressed in this graph and subsequent in litres per second (l/s)

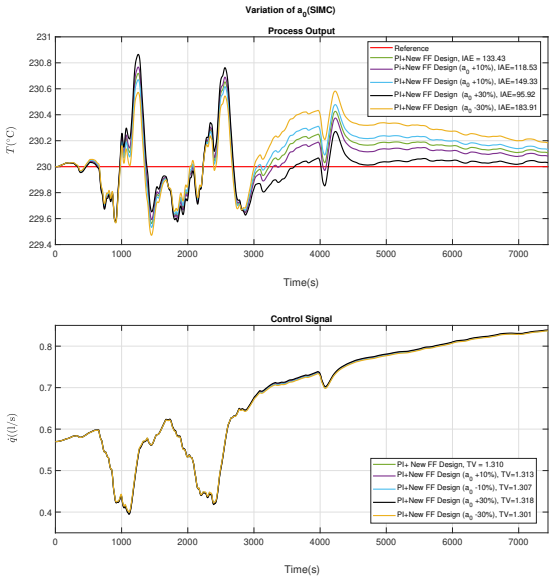


Fig. 4. Comparison of Control Schemes for Temperature Regulation using SIMC Tuning

results in a more conservative evolution of the output temperature, with less notable temperature variations, slower action, and less pronounced oscillations. The third scheme, the improved feedforward, avoids this undesired effect on the control signal, as in the previous case without excessively penalising the reference tracking.

The addition of the four scheme, which incorporates the new feedforward proposal, leads to a significant reduction in oscillations in the control signals. Fig. 5 illustrates a decrease in these oscillations in the case of reference tracking, resulting in improved reference compliance. Regardless of the adjustment method used for the controller, the IAE shows that the feedforward design suggested in this study demonstrates greater efficiency in suppressing disturbances and results in a lower steady-state error at the output. Furthermore, this design prevents the generation of an aggressive control signal that is observed when the feedforward lead-lag scheme is incorporated into the control system.

## 5. CONCLUSION

In this work, we present an innovative feedforward control strategy tailored to distributed parameter systems and highlight its effectiveness in disturbance rejection. Using both the transfer functions derived from the reaction curve method and those obtained from the linear model based on the semi-physical nonlinear model, it is verified that the implementation of feedforward control from the functions derived from the linear model exhibits superior performance in benchmark tracking. This approach demonstrates an effective reduction of oscillations in the control signal compared to conventional feedforward designs. In addition, it significantly improves system performance in the presence of disturbances, addressing, in particular, the dynamics at medium and high frequencies.

Future work will aim to design filters for higher frequencies to eliminate resonances in the frequency response. The

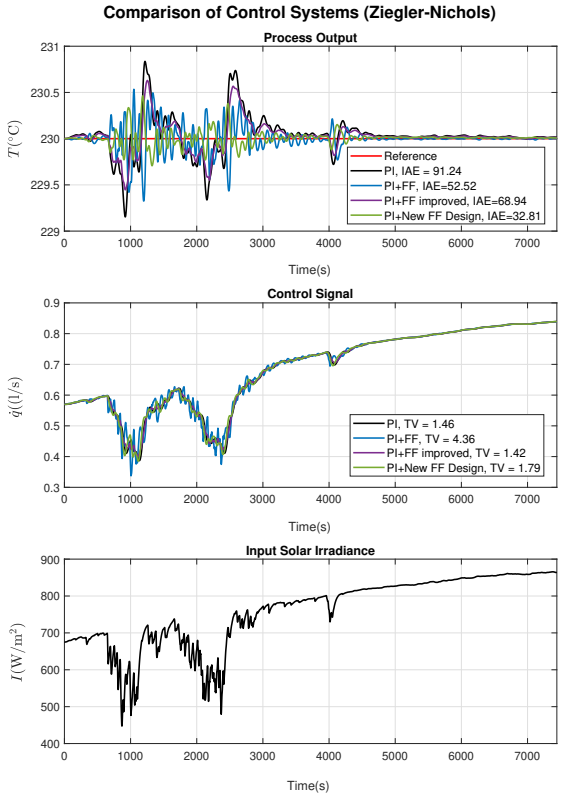


Fig. 5. Comparison of Control Schemes for Temperature Regulation using Ziegler-Nichols Tuning

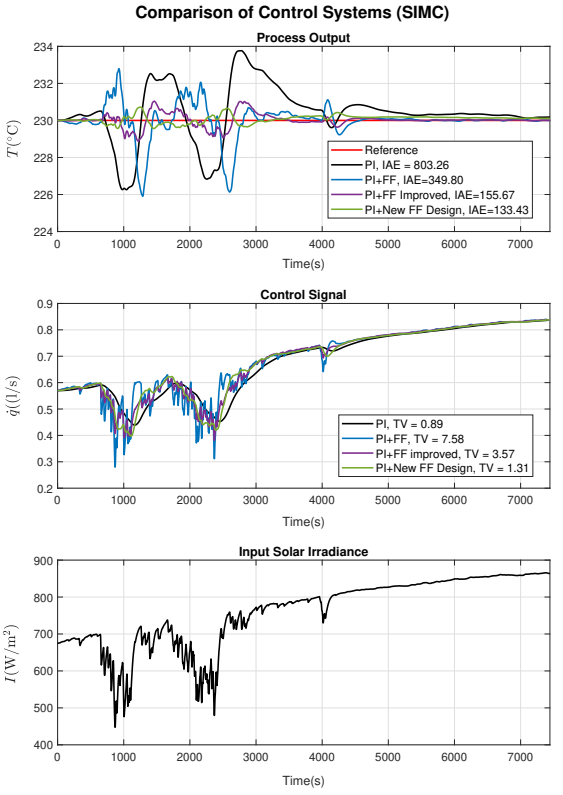


Fig. 6. Comparison of Control Schemes for Temperature Regulation using SIMC Tuning

objective is to verify whether this modification contributes to a resonance-free frequency response, with the aim of improving the system's disturbance rejection capability and reference tracking.

## ACKNOWLEDGEMENTS

This work has been funded by the National R+D+i Plan Project PID2021-126889OB-I00 of the Spanish Ministry of Science and Innovation and EIE funds.

## REFERENCES

Álvarez, J., Yebra, L., and Berenguel, M. (2009). Adaptive repetitive control for resonance cancellation of a distributed solar collector field. *International Journal of Adaptive Control and Signal Processing*, 23, 331 – 352.

Álvarez, J., Normey-Rico, J., and Berenguel, M. (2012). Design of pid controller with filter for distributed parameter systems. *IFAC Proceedings Volumes*, 45(3), 495–500. 2nd IFAC Conference on Advances in PID Control.

Åström, K.J. and Hägglund, T. (2009). *Control PID avanzado*. Pearson, Madrid.

Camacho, E., Rubio, F., Berenguel, M., and Valenzuela, L. (2007). A survey on control schemes for distributed solar collector fields. part i: Modeling and basic control approaches. *Solar Energy*, 81, 1240–1251.

Cohen, W. and Johnston, E. (1956). Dynamic characteristics of double-pipe heat exchangers. *Industrial and Engineering Chemistry*, 48, 1031–1034.

Curtain, R.F. and Morris, K.A. (2009). Transfer functions of distributed parameter systems: A tutorial. *Automatica*, 45, 1101–1116.

Guzmán, J. and Hägglund, T. (2011). Simple tuning rules for feedforward compensators. *Journal of Process Control*, 21(1), 92–102.

Johansen, T.A., Hunt, K.J., and Petersen, I. (2000). Gain-scheduled control of a solar power plant. *Control Engineering Practice*, 8(9), 1011–1022.

Rivera, D., Morarl, M., and Skogestad, S. (1986). Internal model control: Pid controller design. *Industrial and Engineering Chemistry Process Design and Development*, 25, 252–265.

Skogestad, S. (2003). Simple analytic rules for model reduction and pid controller tuning. *Journal of Process Control*, 13(4), 291–309.

Song, X., Wang, M., Ahn, C.K., and Song, S. (2020). Finite-time $\mathscr{H}_\infty$ asynchronous control for nonlinear markov jump distributed parameter systems via quantized fuzzy output-feedback approach. *IEEE Transactions on Cybernetics*, 50(9), 4098–4109.

Ziegler, J. and Nichols, N. (1942). Optimum settings for automatic controllers. *Transactions of the ASME*, 64, 1240–1251.